Impact Factor:					
	ISRA (India) = 4.971	SIS (USA) = 0.912	ICV (Poland) = 6.630
	ISI (Dubai, UAE) = 0.829	РИНЦ (Russia) = 0.126	PIF (India) = 1.940
	GIF (Australia) = 0.564	ESJI (KZ) = 8.716	IBI (India) = 4.260
	JIF = 1.500	SJIF (Morocco) = 5.667	OAJI (USA) = 0.350

SOI: 1.1/TAS DOI: 10.15863/TAS

International Scientific Journal

Theoretical & Applied Science

p-ISSN: 2308-4944 (print) **e-ISSN:** 2409-0085 (online)

Year: 2020 **Issue:** 02 **Volume:** 82

Published: 28.02.2020 **http://T-Science.org**

QR – Issue QR – Article

Denis Chemezov
Vladimir Industrial College
M.Sc.Eng., Corresponding Member of International Academy of Theoretical and Applied Sciences, Lecturer, Russian Federation
https://orcid.org/0000-0002-2747-552X
chemezov-da@yandex.ru

Alexey Kuzin
Vladimir Industrial College
Student, Russian Federation

Daniil Zavyazochnikov
Vladimir Industrial College
Student, Russian Federation

Kirill Khristoforov
Vladimir Industrial College
Student, Russian Federation

Gleb Pisarev
Vladimir Industrial College
Student, Russian Federation

Nikita Putikov
Vladimir Industrial College
Student, Russian Federation

Ivan Gavrilenko
Vladimir Industrial College
Student, Russian Federation

Andrey Gradnikov
Vladimir Industrial College
Student, Russian Federation

THE QUASI-EQUILIBRIUM AND NON-EQUILIBRIUM CRYSTALLIZATION MODELS OF METAL ALLOYS

Abstract: *Comparison of the shrinkage value of iron-based and non-ferrous metal alloys in the conditions of melts crystallization when using the quasi-equilibrium and non-equilibrium models was performed in the article. The ratios coefficients of cooling rates of alloys when the quasi-equilibrium and non-equilibrium crystallization models were obtained.*

Key words: *shrinkage, cooling, alloy, the quasi-equilibrium and non-equilibrium crystallization models.*

Language: *English*

Citation: Chemezov, D., et al. (2020). The quasi-equilibrium and non-equilibrium crystallization models of metal alloys. *ISJ Theoretical & Applied Science, 02 (82),* 130-134.

Soi: http://s-o-i.org/1.1/TAS-02-82-24 ***Doi***: https://dx.doi.org/10.15863/TAS.2020.02.82.24
Scopus ASCC: *2506.*

Introduction

Crystallization of metal alloys in the various casting methods occurs in the certain temperature ranges: from the liquidus temperature (T_{liq}) to the solidus temperature (T_{sol}). The combination of the liquid and solid phases is formed in this range. The solid phase is in equilibrium with the liquid phase. This is due to low diffusion and convection of particles in alloy during cooling. The two-phase zone is described by sum of the several functions (bulk particles of the solid and liquid phases, voids when changing coordinates and time), which vary from 0 to 1. This is the main data for the quasi-equilibrium crystallization model of metal alloys.

The non-equilibrium crystallization model takes into account isolation of the various solid phases during solidification. The crystallization process occurs in the range from T_{liq} to T_{sol}, and below T_{sol}.

Comparison of the quasi-equilibrium and non-equilibrium crystallization models will determine the ratio of changing cooling rates of melts in the mold and the predicted value of the casting shrinkage.

Materials and methods

Shrinkage and cooling rate of various metal alloys in the metal mold were determined. The calculation was performed when using the quasi-equilibrium and non-equilibrium crystallization models. The initial data for the experiment implementation were accepted: *alloy steel* – Fe (97.04%), C (0.4%), Si (0.27%), Mn (0.65%), Cr (0.95%), P (0.035%), S (0.035%), Cu (0.3%), Ni (0.3%), Al (0.02%), CLF up (70%), CLF down (30%), T_0 (1590 °C), T_{liq} (1491.906 °C), T_{sol} (1424.209 °C), T_{eut} (1149.479 °C), Q_{cr} (276 kJ/kg), Q_{eut} (238.468 kJ/kg); *carbon steel* – Fe (98.19%), C (0.2%), Si (0.27%), Mn (0.5%), Cr (0.25%), P (0.035%), S (0.035%), Cu (0.25%), Ni (0.25%), Al (0.02%), CLF up (70%), CLF down (30%), T_0 (1610 °C), T_{liq} (1512.896 °C), T_{sol} (1472.422 °C), T_{eut} (1142.583 °C), Q_{cr} (271 kJ/kg), Q_{eut} (236.127 kJ/kg); *chromium steel* – Fe (85.74%), Cr (12.9%), Ni (0.12%), Si (0.54%), Mn (0.48%), C (0.07%), Cu (0.1%), Mo (0.02%), P (0.02%), S (0.01%), CLF up (70%), CLF down (30%), T_0 (1590 °C), T_{liq} (1493.848 °C), T_{sol} (1490.1 °C), T_{eut} (1478.313 °C), Q_{cr} (304 kJ/kg), Q_{eut} (304 kJ/kg); *corrosion-resistant steel* – Fe (69.75%), Ni (9%), Cr (18%), Si (0.5%), Mn (1.5%), C (0.12%), Cu (0.1%), Ti (1%), P (0.02%), S (0.01%), CLF up (70%), CLF down (30%), T_0 (1540 °C), T_{liq} (1447.05 °C), T_{sol} (1388.766 °C), T_{eut} (1346.803 °C), Q_{cr} (259 kJ/kg), Q_{eut} (259 kJ/kg); *malleable cast iron* – Fe (93.58%), C (3.6%), Si (2.5%), Mn (0.1%), P (0.02%), S (0.01%), Cu (0.15%), Mg (0.04%), CLF up (70%), CLF down (30%), T_0 (1250 °C), T_{liq} (1157.94 °C), T_{sol} (1150.51 °C), T_{eut} (1150.421 °C), Q_{cr} (160 kJ/kg), Q_{eut} (254.52 kJ/kg); *grey cast iron* – Fe (93.67%), C (3.35%), Si (2.05%), Mn (0.7%), P (0.15%), S (0.08%), CLF up (50%), CLF down (30%), T_0 (1270 °C), T_{liq} (1178.297 °C), T_{sol} (1150.075 °C), T_{eut} (1150.064 °C), Q_{cr} (160 kJ/kg), Q_{eut} (257.053 kJ/kg); *white cast iron* – Fe (63.25%), C (3%), Si (0.7%), Mn (0.6%), Cr (31%), P (0.1%), S (0.1%), Ni (1.25%), CLF up (70%), CLF down (30%), T_0 (1400 °C), T_{liq} (1306.389 °C), T_{sol} (1236.225 °C), T_{eut} (1236.183 °C), Q_{cr} (160 kJ/kg), Q_{eut} (242.99 kJ/kg); *silumin* – Al (87.81%), Si (11.5%), Mn (0.08%), Cu (0.1%), Fe (0.5%), Ti (0.01%), CLF up (70%), CLF down (30%), T_0 (690 °C), T_{liq} (596.798 °C), T_{sol} (576.09 °C), T_{eut} (576.09 °C), Q_{cr} (340 kJ/kg), Q_{eut} (505.611 kJ/kg); *brass* – Cu (60%), Zn (40%), CLF up (70%), CLF down (30%), T_0 (990 °C), T_{liq} (898.128 °C), T_{sol} (890.954 °C), T_{eut} (419 °C), Q_{cr} (136 kJ/kg), Q_{eut} (136 kJ/kg); *magnesium alloy* – Mg (93.4%), Al (3.1%), Mn (0.5%), CLF up (70%), CLF down (30%), T_0 (730 °C), T_{liq} (632.002 °C), T_{sol} (586.577 °C), T_{eut} (390.66 °C), Q_{cr} (293.6 kJ/kg), Q_{eut} (363.842 kJ/kg); *nickel alloy* – Ni (62.785%), Cr (9.5%), Al (4.4%), Co (13.5%), Ti (5.3%), W (1.4%), Mo (3%), B (0.15%), C (0.1%), CLF up (70%), CLF down (30%), T_0 (1380 °C), T_{liq} (1282.978 °C), T_{sol} (1267.638 °C), T_{eut} (1223.505 °C), Q_{cr} (297.4 kJ/kg), Q_{eut} (293.709 kJ/kg); *nickel-cobalt alloy* – Ni (80%), Co (20%), CLF up (70%), CLF down (30%), T_0 (1560 °C), T_{liq} (1465.682 °C), T_{sol} (1460.6 °C), T_{eut} (1452 °C), Q_{cr} (270 kJ/kg), Q_{eut} (270 kJ/kg); *tin bronze* – Cu (91%), Sn (9%), CLF up (70%), CLF down (30%), T_0 (1110 °C), T_{liq} (1014.631 °C), T_{sol} (862.914 °C), T_{eut} (227 °C), Q_{cr} (175.7 kJ/kg), Q_{eut} (175.7 kJ/kg); *tinless bronze* – Cu (95%), Al (5%), CLF up (70%), CLF down (30%), T_0 (1160 °C), T_{liq} (1062.592 °C), T_{sol} (1058.225 °C), T_{eut} (1037 °C), Q_{cr} (197.5 kJ/kg), Q_{eut} (296.9 kJ/kg); *zinc alloy* – Zn (72.65%), Al (25%), Mg (0.1%), Cu (2.25%), Fe (0.7%), Pb (0.1%), Cb (0.1%), CLF up (30%), CLF down (30%), T_0 (580 °C), T_{liq} (489.378 °C), T_{sol} (377.686 °C), T_{eut} (377.685 °C), Q_{cr} (180 kJ/kg), Q_{eut} (123.269 kJ/kg).

Results and discussion

The experiment results were presented graphically. Two dependencies were built for comparison of the quasi-equilibrium and non-equilibrium crystallization models of metal alloys.

The dependencies of changing shrinkage of iron-based alloys from melt cooling rate are presented in the Fig. 1.

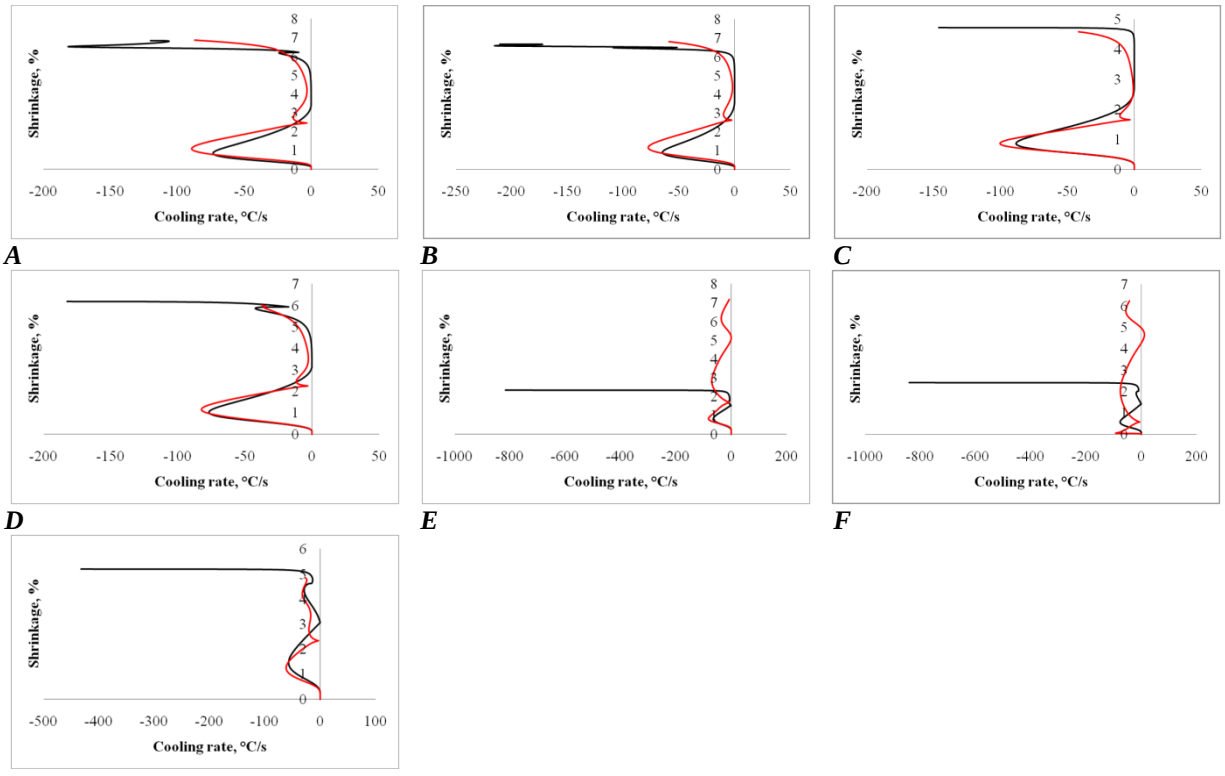

Figure 1 – The dependencies of changing shrinkage of iron-based alloys from melt cooling rate: *A* – alloy steel, *B* – carbon steel, *C* – chromium steel, *D* – corrosion-resistant steel, *E* – malleable cast iron, *F* – grey cast iron, *G* – white cast iron. — the quasi-equilibrium crystallization model, — the non-equilibrium crystallization model.

Cooling rate of steels at the end of the crystallization process when using the quasi-equilibrium model is several times higher than cooling rate of steels at the end of the crystallization process when using the non-equilibrium model. Shrinkage of steels when the quasi-equilibrium and non-equilibrium crystallization models is almost the same. Maximum cooling rate is observed during crystallization of carbon steel.

Malleable and grey cast irons have different cooling rates. Maximum cooling rate (over 800 °C/s) is observed for cast irons at the end of the crystallization process when using the quasi-equilibrium model. Cooling rate of grey and malleable cast irons was determined in the range of 0-100 °C/s when the non-equilibrium crystallization model. Shrinkage of cast irons when the quasi-equilibrium crystallization model is 2.5-3 times less than when the non-equilibrium crystallization model. Calculated shrinkage for the two models is the same after crystallization of white cast iron.

Cooling rate of iron-based alloys has the negative values (the temperature decreases) in all cases, except for grey cast iron (the temperature of alloy increases at the certain phase section).

The dependencies of changing shrinkage of non-ferrous metal alloys from melt cooling rate are presented in the Fig. 2.

Cooling rates when using the considered crystallization models are different for non-ferrous metal alloys:

- maximum cooling rate of magnesium and zinc alloys is observed at the beginning of the crystallization process when using the non-equilibrium model;
- minimum cooling rate of nickel-cobalt alloy and tinless bronze is determined when the non-equilibrium crystallization model;
- increasing the temperature during cooling occurs only when the non-equilibrium crystallization model (brass, magnesium and zinc alloys).

The shrinkage value of non-ferrous metal alloys after crystallization is different for the two models. Shrinkage of alloys is less in the conditions of the non-equilibrium crystallization model.

The calculated values of the ratios coefficients of cooling rates of alloys when the quasi-equilibrium and non-equilibrium crystallization models are presented in the table 1.

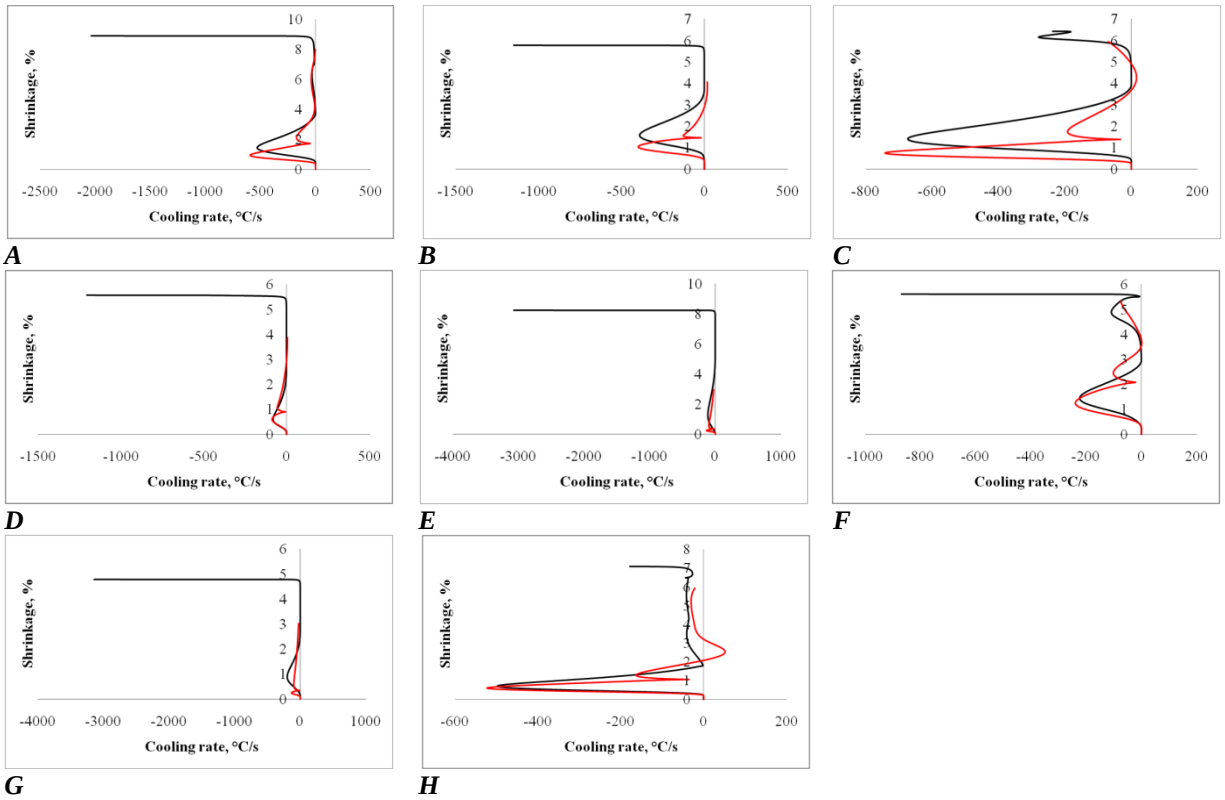

Figure 2 – The dependencies of changing shrinkage of non-ferrous metal alloys from melt cooling rate: *A* – silumin, *B* – brass, *C* – magnesium alloy, *D* – nickel alloy, *E* – nickel-cobalt alloy, *F* – tin bronze, *G* – tinless bronze, *H* – zinc alloy. — the quasi-equilibrium crystallization model, — the non-equilibrium crystallization model.

Table 1. The ratios coefficients of cooling rates of alloys when the quasi-equilibrium and non-equilibrium crystallization models.

Alloy	Coefficient
Alloy steel	-0.7166666666666666666337
Carbon steel	-4.448979591836734693860644897959 2
Chromium steel	0.6325088339222614841006477031802 1
Corrosion-resistant steel	4.9999999999999999949675
Malleable cast iron	-105.6666666666666666645639
Grey cast iron	24999.999999999
White cast iron	-1.2394366197183098592156619718 31
Silumin	2.3333333333333333333034666666667
Brass	0.9661016949155923728948813559321 9
Magnesium alloy	3.1052631578947368421145789473684
Nickel alloy	16.3333333333333333333398666666667
Nickel-cobalt alloy	4.6249999999999999998335
Tin bronze	-1.9354838709677419354412903225806
Tinless bronze	5.9230769230769230769230769230769
Zinc alloy	0.9859154929577464789097183098591 5

The significant changing ranges of cooling rates are dominated in grey and malleable cast irons in comparing the two considered crystallization models. The negative value of the coefficient indicates the positive and negative values of cooling rate of alloys for the two considered crystallization models.

Conclusion

1. Cooling rate and the shrinkage value of malleable and grey cast irons when the quasi-equilibrium and non-equilibrium crystallization models are different and vary several times. Almost identical cooling rates are observed during crystallization of steels.

2. It is determined that the cooling temperature increases over the certain time range during non-equilibrium crystallization of grey cast iron, brass, magnesium and zinc alloys.

3. The ratios of cooling rates of corrosion-resistant steel and nickel-cobalt alloy, brass and zinc alloy during quasi-equilibrium and non-equilibrium crystallization are almost the same.

References:

1. Brimacombe, J. K. (1993). Intelligent mould for continuous casting of billets. *Metall. Trans, B24*, 917-928.
2. Nakagawa, T., Umeda, T., & Murate, T. (1995). Strength and ductility of solidifying shell during casting. *Trans. Iron Steel Inst. Jap*, *35*, 723-728.
3. Ray, S. K., Mukhopadhyay, B., & Das, P. C. (1999). Effect of chemistry on solidification and quality of stainless steel. *Presented at Annu. Tech. Mtg. of Indian Inst. Metals*.
4. Langford, G., & Cunningham, R. E. (1978). Steel casting by diffusion solidification. *Springer Science and Business Media LLC in Metallurgical and Materials Transactions A Metallurgical and Materials Transactions A, Volume 9*, 5-19.
5. Chemezov, D., Bayakina, A., Bogomolova, E., & Lukyanova, T. (2017). To the question of the solidification process of steel castings with different wall thicknesses. *ISJ Theoretical & Applied Science, 03 (47)*, 38-41.
6. Chemezov, D. (2017). Stress fields in a steel casting. *ISJ Theoretical & Applied Science, 05 (49)*, 165-172.
7. Chemezov, D., Bakhmeteva, M., Bayakina, A., Polushin, V., Lukyanova, T., & Igumentseva, A. (2017). Analysis of the manufacturing process of the case-shaped casting in the sand mould. *ISJ Theoretical & Applied Science, 06 (50)*, 14-52.
8. Chemezov, D. (2017). Shrinkage of some metal alloys after solidification. *ISJ Theoretical & Applied Science, 06 (50)*, 87-89.
9. Chemezov, D. (2017). The degree of shrinkage porosity in the castings after solidification. *ISJ Theoretical & Applied Science, 07 (51)*, 1-6.
10. Chemezov, D. (2017). Convective heat transfer when cooling of metallic melts. *ISJ Theoretical & Applied Science, 09 (53)*, 1-7.
11. Chemezov, D. (2017). The mathematical models of shrinkage formation in metallic alloys. *ISJ Theoretical & Applied Science, 09 (53)*, 23-42.
12. Chemezov, D., Bayakina, A., & Lukyanova, T. (2017). Residual stresses in silumin after high-pressure die casting. *ISJ Theoretical & Applied Science, 11 (55)*, 1-8.
13. Chemezov, D., Smirnova, L., & Bogomolova, E. (2018). Metal mold casting of cast iron and aluminium pistons. *ISJ Theoretical & Applied Science, 05 (61)*, 132-141.
14. Chemezov, D. (2018). Condition of a casting material of a cylinder block of a car after crystallization in a sand mold. *ISJ Theoretical & Applied Science, 07 (63)*, 145-147.
15. Chemezov, D., Pavluhina, I., Komissarov, A., & Kanishchev, I. (2019). Properties research of grey cast iron in condition of gravity casting into a metal mold. *ISJ Theoretical & Applied Science, 07 (75)*, 1-4.
16. Chemezov, D., et al. (2019). Influence of a mold material and percentage of chemical elements in melt on shrinkage of steel and cast iron castings. *ISJ Theoretical & Applied Science, 10 (78)*, 301-306.
17. Chemezov, D., et al. (2019). Influence of a mold material and percentage of chemical elements in melt on shrinkage of castings made of nonferrous metals alloys. *ISJ Theoretical & Applied Science, 10 (78)*, 401-406.
18. Chemezov, D., et al. (2019). The calculated deformed volume of the brake drum casting of the car. *ISJ Theoretical & Applied Science, 12 (80)*, 152-154.